

# Isolated Shoot-Through Z-Source Inverter

Huaqiang Zhang<sup>1</sup>, Caijuan Qi<sup>1</sup>, Jian Zhang<sup>1</sup>, Lingshun Liu<sup>2</sup>

1. Department of Electrical Engineering, Harbin Institute of Technology at Weihai, Weihai Shandong 264209, China;

2. Department of Control Engineering, Naval Aeronautical and Astronautical University, Yantai Shandong 264001, China

**Abstract** — The boost factor and modulation index of traditional Z source inverter restrains each other and the inserted shoot-through duty ratio must be less than the zero vector in a switch cycle. These defects not only limit boost capability but also reduce the flexibility of control strategy. An isolated shoot-through Z-source inverter (IST-ZSI) topology structure which adding a diode, a capacitor and an entirely-controllable device in traditional impedance network is proposed. The inverter reduces the starting-up inrush current and the voltage stress on capacitors greatly, separates the control of shoot-through duty ratio from the topology, which realizes the decoupling control between boost factor and modulation index, and obtains higher voltage transfer ratio and good dynamic performance. On the base of theoretical analysis, the simulation and experiment on IST-ZSI have been done. The research results verify the correctness and the superiority of the topology.

**Key words:** Z-source inverter; isolated; decoupling control; boost capability; shoot-through zero vector

## I. INTRODUCTION

In 2002, the topology of Z-source inverter was proposed. The uniqueness of this topology lies in the introduction of Z-source network which can make the upper and lower devices of each phase leg gate on simultaneously. This shoot-through state provides a single-stage buck-boost function. Therefore, Z-source inverter has many important research and application values, such as in renewable energy connected to power grid [1-3], in electric vehicles [4, 5], in motor drive [6, 7] etc. In recent years, different aspects of Z-source inverter have been studied by scholars from all over the world. [8-9] presented a three-level Z-source inverter, suitable for high voltage and high power occasion. A double-output Z-source inverter was summarized in [10], which can increase the number of loads, and fit the conditions of multiple loads and large gap of output voltage. In view of the shortcomings of Z-source inverter, a quasi-Z-source inverter was proposed in [11]. On the basis of quasi-Z-sources, a new T-source inverter, introducing a coupling transformer and reducing a capacitor, was proposed in [12], which not only had good boost capability, but used fewer devices and had small size and low cost. A tapped inductor quasi-Z-source inverter was put forward in [13], which provided high inversion gain, but was difficult to avoid the adverse effects of leakage inductance. In order to increase the boost capability of traditional Z-source inverter, a switch inductor Z-source

The authors thank the support both the Foundation of National Natural Science (51377168) and the Foundation of Shandong Province Science and Technology Development Planning (2011GGH20411), which enabled the achievement of the mentioned research results.

inverter was proposed in [14], however, the proposed inverter led to the problems of more devices, larger volume and higher cost.

To some extent, though the performance of Z-source inverter is improved by many improved programs, there are still a number of substantive issues unsolved. For example, due to the pinning and coupling of boost factor ( $B$ ) and modulation index ( $M$ ) in traditional Z-source inverter, the way of improving boost capability is restricted. But, the high boost inversion abilities of Z-source inverter must be required in the condition of low-voltage input. In this paper an isolated shoot-through Z-source inverter (IST-ZSI) is proposed for this problem. Compared to traditional Z-source inverter, this topology has many advantages. It can be summarized in the following.

- 1) The control of shoot-through duty ratio is separated from the topology, which can obtain high boost capability by increasing shoot-through duty ratio.
- 2) Avoiding the problem of serious starting-up inrush current and high capacitor voltage stress.
- 3) Overcome the mutual coupling of boost factor and modulation index, and realize the flexible control of shoot-through duty ratio from 0 to 50% without the limitation of zero vectors in SPWM or SVPWM algorithm.

On the foundation of Z-source inverter and their families, theoretical analysis and experimental verification of IST-ZSI have been done in this paper. The research results verify the aforementioned advantages.

## II COMPARISON OF SEVERAL Z-SOURCE INVERTERS BOOST CONTROL

As shown in Fig. 1, the impedance network of traditional Z-source inverter connected in X-shape couples input source and inverter, which has buck-boost function.

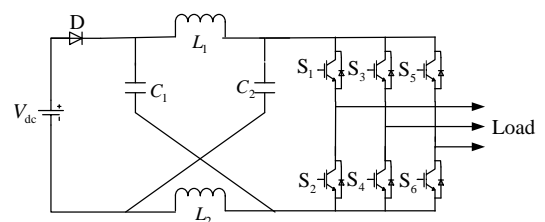


Fig.1. Topology of traditional Z-source inverter.

The operation principles of Z-sources inverter have been analyzed in [15], which achieve boost capability by controlling the shoot-through duty ratio. The boost factor of Z-source network can be expressed as

$$B = \frac{1}{1-2D} \tag{1}$$

where  $D$  is shoot-through duty ratio.

The capacitors voltage of Z-source network and the output peak phase voltage from the inverter can be respectively expressed as

$$V_c = \frac{1-D}{1-2D} V_{dc} \tag{2}$$

$$V_g = \frac{MB}{2} V_{dc} = GV_{dc} \tag{3}$$

where  $M$  is the modulation index, and  $G$  is the voltage gain of Z-source inverter.

The Z-source inverter overcomes the limitations of traditional voltage-source inverter and current-source inverter and provides a novel power conversion concept. However, the traditional Z-source inverter still shows some drawbacks, such as: the discontinuous input current, serious starting-up inrush current, high capacitor voltage stress of the impedance network, limited shoot-through duty ratio and the mutual coupling relationship between  $B$  and  $M$  etc. The reason why the boost factor  $B$  coupled with modulation index  $M$  is that the boost ratio of Z-source inverter is determined by shoot-through duty ratio which is determined by the zero vector in a switching cycle, while the modulation index determines the remaining zero vector duty ratio. Therefore,  $B$  increases with the decrease of  $M$ , which also reduces the flexibility of the control strategy. Here, we take the traditional synchronized pulse width modulation (SPWM) control strategy as the example, for fixed modulation index  $M$ , the remaining zero vector duty ratio of a switching cycle is  $1-M$ , so the maximum shoot-through duty ratio can be expressed as  $D=1-M$ , namely, to get a larger shoot-through duty ratio  $D$  is bound to reduce the modulation index  $M$  [16].

For these problems, scholars have proposed varies of quasi-Z-source inverters (qZSI). As shown in Fig. 2(a), single-stage qZSI was proposed in [17-19]. The difference of the improved Z-source inverter is that the positions of the inverter bridge and diode are exchanged, which effectively solve huge starting-up inrush current and high capacitor voltage stress, however, the biggest drawback is the limited boost ratio, which is hard to meet the occasion of wide input voltage. Based on the aforementioned, improved multistage qZSI was put forward in [20, 21], which can be divided into three categories: diode-assisted extended-boost, capacitor-assisted extended-boost and hybrid extended-boost, as shown in Fig. 2(b), Fig. 2(c) and Fig. 2(d), respectively. For diode-assisted extended-boost qZSI, a inductor, a capacitor and two diodes are added while boost ratio becomes original  $1/(1-D)^2$  times. For capacitor-assisted extended-boost qZSI, a inductor, two capacitors and a diode are added while boost ratio becomes  $1/(1-(2+N)*D)$  (where  $N$  is the number of increased stages).

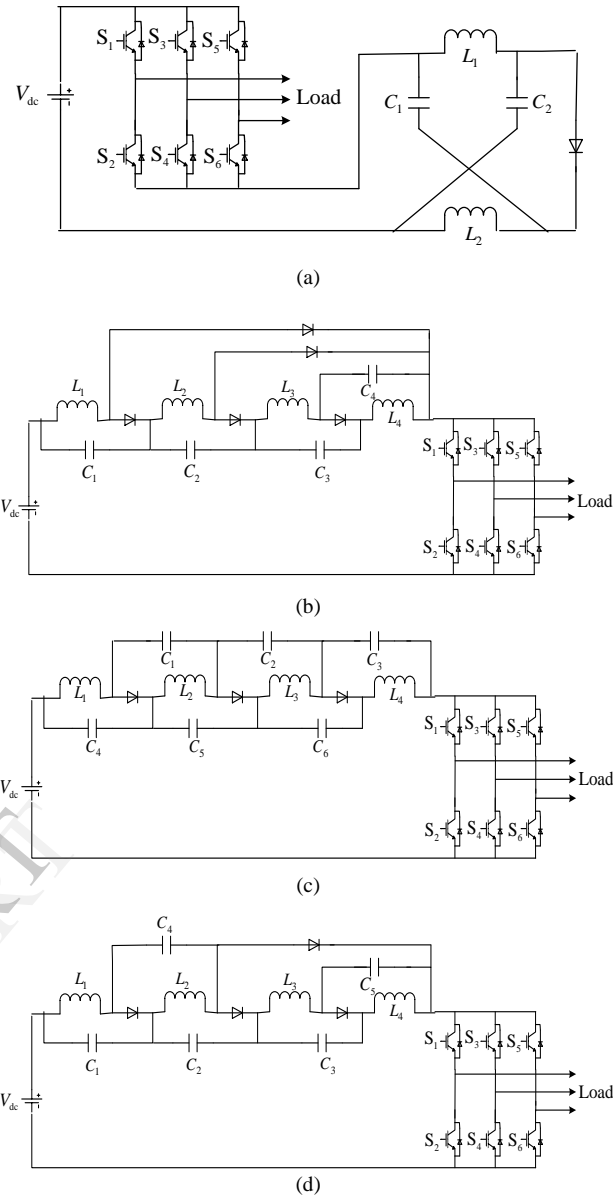


Fig.2. Improved quasi-Z-source inverter. (a) Single-stage quasi-Z-source inverter; (b) Diode-assisted extended-boost qZSI; (c) Capacitor-assisted extended-boost qZSI; (d) Hybrid extended-boost qZSI.

As shown in Fig. 2 (b), the boost factor can be expressed as

$$B = \frac{1}{(1-2D)(1-D)^2} \tag{4}$$

In Fig. 2 (c) the boost factor can be expressed as

$$B = \frac{1}{(1-4D)} \tag{5}$$

As we can see from (4) and (5), no matter diode-assisted extended-boost or capacitor-assisted extended-boost, it could improve boost factor by cascade, and need less shoot-through duty ratio when achieving the same boost ratio. Although it improves boost capability greatly, but simultaneously, more devices are applied. Furthermore, with the increasing number

of extended-stage, more devices are needed, thus it leads to the problem of complex structure, high cost and large volume etc.

In addition, too small shoot-through duty ratio is susceptible to be interfered by system, which will cause system instability. More importantly, these structures do not solve the drawback of the coupling relationship between  $B$  and  $M$ , and the control flexibility is inadequate, thus the application areas of Z-source inverter are limited, especially, in high boost ratio occasion.

### III. ISOLATED SHOOT-THROUGH Z-SOURCE INVERTER

#### A. Circuit Topology

The topology of isolated shoot-through Z-source inverter (IST-ZSI) is shown in Fig. 3. Its basic idea is that the traditional Z-source network and the inverter are separated by an independent circuit, which consists of an IGBT, a diode and a large capacitor. This circuit realizes the decoupling control of boost factor and modulation index.

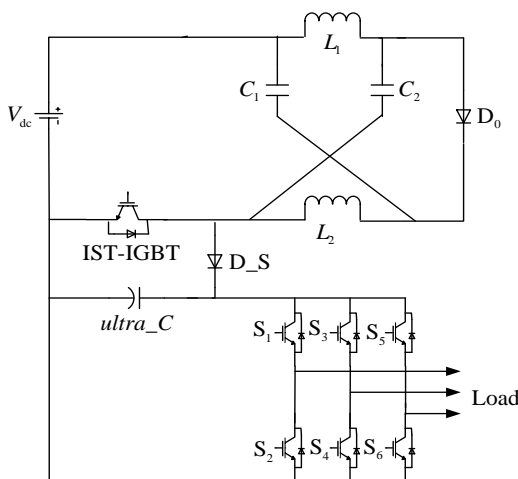


Fig.3. Topology of the isolated shoot-through Z-source inverter (IST-ZSI).

Isolated shoot-through Z-source inverter adds a full-controlled device IGBT in traditional Z-source inverter, which individually controls the shoot-through duty ratio, the IGBT is designated as IST-IGBT. Meanwhile a large capacitor ( $ultra\_C$ ) is connected in DC-link, which is used to gentle the fluctuation of DC-link voltage after joining shoot-through duty ratio and has the ability to provide instant high current. In order to avoid  $ultra\_C$  through IST-IGBT discharges in shoot-through state, it is necessary to add a diode between IST-IGBT and  $ultra\_C$ . This diode mainly plays the role of separating IST-IGBT and  $ultra\_C$ , so we call it  $D_S$ . This topology decouples boost factor and modulation index, and the shoot-through duty ratio is separated from physical structure, thus, the inverter is termed isolated shoot-through Z-source inverter.

#### B. Operation Principles

From the view point of the switching states of the main circuit, the operation principles of IST-ZSI are similar to those traditional Z-source inverters. The substates of the proposed topology are classified into the shoot-through state and the non-shoot-through state, respectively.

1) *Shoot-Through State*: IST-IGBT is on, and its

equivalent circuit is shown in Fig. 4(a). In this state, IST-IGBT, DC power source and the two inductors  $L_1$  and  $L_2$  form a closed circuit. Meanwhile, the two inductors get charged, then, the charged inductors can be regard as DC source. Assuming that the inductors  $L_1$  and  $L_2$  and the capacitors  $C_1$  and  $C_2$  have the same inductance ( $L$ ) and capacitance ( $C$ ), respectively, we have

$$\begin{cases} V_{C1} = V_{C2} = V_C \\ V_{L1} = V_{L2} = V_L \end{cases} \quad (6)$$

When in the shoot-through state, the inductors of Z-source network get charged and the capacitors discharge, we can get

$$\begin{cases} V_L = V_{dc} + V_C \\ U_o = 0 \end{cases} \quad (7)$$

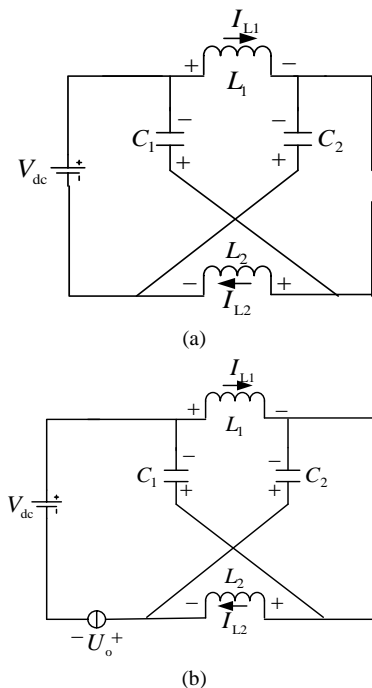


Fig.4. Equivalent circuits of isolated shoot-through Z-source inverter. (a) Shoot-through state; (b) Non-shoot-through state.

2) *Non-Shoot-Through State*: IST-IGBT is off, and its equivalent circuit is shown in Fig. 4(b). In this state,  $V_{dc}$  and equivalent DC source of the inductors supply loads together.

It can be seen from Fig. 4(b) that during non-shoot-through state, the inductors of Z-source network discharge, the capacitors get charged and the diode  $D_0$  is positive onset. By applying KVL, the following steady-state relationships can be observed

$$\begin{cases} V_L = -V_C \\ U_o = V_{dc} + V_C - V_L = V_{dc} + 2V_C \end{cases} \quad (8)$$

Considering the fact that the average voltage of the inductors over one switching period should be zero in steady state, thus, the following relationship can be derived

$$V_c = \frac{D}{1-2D} V_{dc} \tag{9}$$

Combining expression (8) with expression (9), the DC-link voltage can be described as

$$U_o = \frac{1}{1-2D} V_{dc} = B V_{dc} \tag{10}$$

If under the condition of SVPWM, the output peak phase voltage from the inverter can be expressed as

$$V_g = \frac{U_o}{\sqrt{3}} = \frac{B}{\sqrt{3}} V_{dc} \tag{11}$$

In Fig. 3, the IST-IGBT realizes the independent control of Z-source shoot-through vector, making the control of inverter output is more flexible. Compared to the aforementioned Z-source inverters, IST-ZSI not only has its excellent characteristics, but also realizes the decoupling control of  $B$  and  $M$ , which makes  $B$  can adjust in a large range so that it can get a higher voltage transfer ratio. What's more, the value of shoot-through duty ratio will be not too small and not easy to be interfered by system, so it can obtain stable boost factor  $B$ .

**C. Capacitor voltage stress and the Ability of Soft-start**

From (1)、(2) and (9), we can get the relationship between the ratio of capacitor voltage stress and  $V_{dc}$  ( $V_c/V_{dc}$ ) and boost factor ( $B$ ) in traditional Z-source inverter and IST-ZSI.

In traditional Z-source inverter

$$V_c / V_{dc} = \frac{B+1}{2} \tag{12}$$

In IST-ZSI

$$V_c / V_{dc} = \frac{B-1}{2} \tag{13}$$

The relationship curve is shown in Fig. 5.

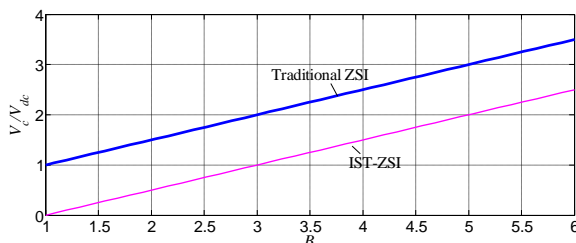


Fig.5. Comparison of capacitor voltage stress between traditional Z-source inverter and IST-ZSI.

It can be seen from Fig. 5 that the capacitor voltage stress of traditional Z-source network is much higher than IST-ZSI's in the same boost factor. Therefore, to achieve the same gain, IST-ZSI can choose smaller capacity capacitors, which is beneficial to reduce cost and volume.

The capacitor voltage of impedance network is determined by shoot-through duty ratio  $D$ . According to expression (9),

when  $D$  is zero, the corresponding capacitor voltage is also zero. As for the steady increase of shoot-through duty ratio  $D$  from zero to expected value, it could effectively reduce damages to capacitors caused by instantaneous high voltage, thus it achieves the goal of soft-start and small startup current.

**D. Boost Capability Analysis of Inverter**

The boost inversion ability of a whole Z-source is determined by the interactions of Z-source impedance and the PWM control method applied to the main circuit. As described in [22], two kinds of common modulation strategy which termed as the simple boost control method and the third harmonic injection control method have been introduced. The simple boost control method is convenient and simple, and the third harmonic injection method can increase the range of  $M$ , both of which are widely used in three-phase inverter system. Among, the sketch map of third harmonic injection control is shown in Fig. 6.

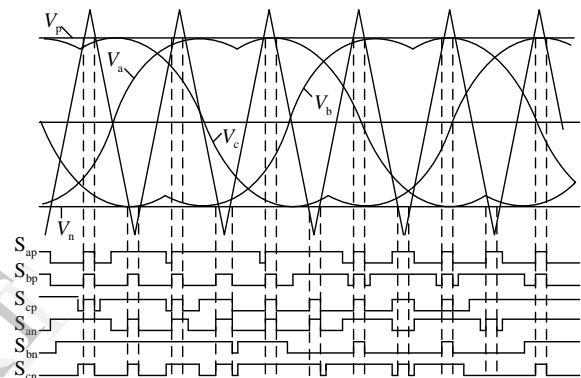


Fig.6. Sketch map of third harmonic injection control.

The relationship of shoot-through duty ratio and modulation index in simple boost control can be expressed as

$$M = 1 - D \tag{14}$$

Combining expression (1) with expression (14), the voltage gain  $G$  can be described as

$$G = \frac{V_g}{V_{dc}} = BM = \frac{1-D}{1-2D} \tag{15}$$

The relationship of  $D$  and  $M$  in third harmonic injection is

$$M = \frac{2\sqrt{3}(1-D)}{3} \tag{16}$$

The voltage gain  $G$  is

$$G = BM = \frac{2\sqrt{3}(1-D)}{3(1-2D)} \tag{17}$$

From (11), the voltage gain of IST-ZSI can be obtained as follows

$$G = \frac{V_g}{\frac{V_{dc}}{2}} = \frac{2}{\sqrt{3}(1-2D)} \quad (18)$$

Based on expression (15), expression (17) and expression (18), the relationship of voltage gain and shoot-through duty ratio is shown in Fig. 7. It can be seen that the voltage gain of IST-ZSI is bigger in the same shoot-through duty ratio. Taking  $D=0.4$  as example, in simple boost control the voltage gain of traditional Z-source inverter is  $G_1=3$ , in third harmonic injection the voltage gain is  $G_2=3.46$  while the IST-ZSI's is  $G=5.77$ . In actual, the shoot-through duty ratio of traditional Z-source inverter is impossible to achieve 30% in general. Because in order to achieve a larger shoot-through duty ratio, the modulation index must be a lower one, which will seriously affect the quality of inverter output voltage. When  $D=0.3$ ,  $G=2$ , i.e. the maximum voltage gain of traditional Z-source inverter is around 2. To IST-ZSI, it has realized the decoupling control of  $B$  and  $M$ , so we need not consider the negative impacts of low modulation index brought in when shoot-through duty ratio is high.

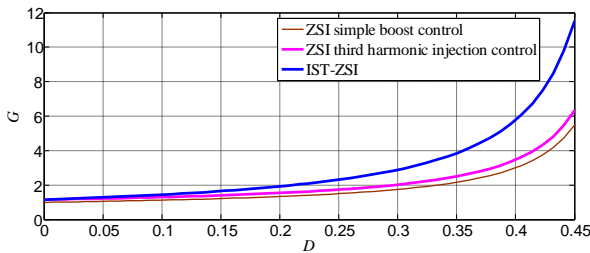


Fig.7. Voltage conversion gain comparison of traditional topology and IST-ZSI in the same shoot-through duty ratio.

### E. The Parameters Design of IST-ZSI

The design of related parameters in IST-ZSI mainly includes the design of Z-source impedance network and the design of *ultra\_C*.

#### 1) The Design of inductors for impedance network

The design of inductors mainly considers if the current continuous or not. If the value of inductors is too small, it will not guarantee the continuity of current. The circuit will enter non-normal state in discontinuous current. If the value of inductors is too big, it will be easy to form resonant with capacitors. The following formula can be selected

$$V_L = L \frac{dI_L}{dt} \quad (19)$$

where

$$dI_L = \Delta I_L = x_1 \% I_L \quad (20)$$

$$dt = \Delta t = DT / n \quad (21)$$

Hence, it can be deduced that

$$L = \frac{V_L dt}{dI_L} = \frac{V_C \Delta t}{\Delta I_L} = \frac{V_C DT}{x_1 \% n I_L} \quad (22)$$

where,  $x_1\%$  is the percentage of current ripple.  $n$  is the number

of shoot-through in a switch cycle, and there is only one shoot-through vector in a switch cycle for IST-ZSI, so  $n=1$ .  $I_L$  denotes the mean value of inductor current, as for the inductor current is equal to the load current, thus the value of  $I_L$  can be determined by the maximum load current.

#### 2) The Design of capacitors for impedance network

The capacitors of impedance network are mainly determined by the ripple of capacitor voltage. If the value of capacitor is too big, its cost and volume will increase. If the value of capacitor is too small, it will not suppress the voltage ripple. Thus, the following equation can be used to select

$$I_C = C \frac{dV_C}{dt} \quad (23)$$

where

$$dV_C = \Delta V_C = x_2 \% V_C \quad (24)$$

$$dt = \Delta t = DT / n \quad (25)$$

From (23) to (25), we can get

$$C = \frac{I_C dt}{dV_C} = \frac{I_L \Delta t}{\Delta V_C} = \frac{I_L DT}{x_2 \% n V_C} \quad (26)$$

where  $x_2\%$  is the percentage of voltage ripple.

#### (3) The Design of *ultra\_C*

The main function of *ultra\_C* is used to gentle the DC-link voltage ripple, which is caused by the shoot-through of IST-IGBT, simultaneously it also provides instantaneous high current.

When capacitor get charged, it satisfies (27)

$$V_t = V_0 + (V_1 - V_0) \times (1 - e^{-\frac{t}{R_0 C}}) \quad (27)$$

where,  $V_0$  is the initial voltage of capacitor.  $V_1$  is the final voltage of capacitor, i.e. the charged voltage of capacitor.  $V_t$  is the capacitor voltage at time  $t$ .  $R_0$  is the resistance of charging circuit.

In the extreme case, the initial voltage of *ultra\_C* is always zero at the beginning of charge, so  $V_0 = 0$ . It can be considered that the charging process is over when the value of *ultra\_C* is up to 95% of the DC-link voltage. Hence,

$$V_t = 0.95 \times \frac{1}{1-2D} V_{dc} \quad (28)$$

While the final value of charge is equal to DC-link voltage, so

$$V_1 = \frac{1}{1-2D} V_{dc} \quad (29)$$

The charging of *ultra\_C* should be completed during the shoot-through time in a switch cycle. Therefore the charging time can be expressed as

$$t = DT \tag{30}$$

From formula (27) to (30), we can get

$$ultra\_C = \frac{DT}{(1 - \ln 0.05) R_0} \tag{31}$$

#### IV SIMULATION ANALYSIS

To verify the aforementioned theoretical results, a simulation example for isolated shoot-through Z-source inverter is given in open-loop mode under the condition of SVPWM. The corresponding parameters are shown in Tab. 1.

Tab.1. Parameters of isolated shoot-through Z-source inverter. (where,  $R_1$  is the protect resistance of  $ultra\_C$ ,  $R$  is the load,  $f_s$  is the frequency of switch)

Parameter	Value	Parameter	Value
$V_{dc}/V$	35	$R_1/\Omega$	0.1
$L/mH$	19.2	$R/\Omega$	10
$C/\mu F$	700	$f_s/kHz$	10
$Ultra\_C/\mu F$	470	$M$	0.84

The comparison of waveforms between IST-ZSI and traditional Z-source inverter with same output voltage can be seen in Fig. 8. Under the condition of third harmonic injection, the same simulation parameters as IST-ZSI are chosen by traditional Z-source inverter. When shoot-through duty ratio  $D=20\%$ , the simulation waveforms of IST-ZSI's Z-source capacitor voltage ( $V_c$ ), DC-link voltage ( $U_o$ ) and inverter output phase voltage ( $V_g$ ) are shown in Fig. 8(a). It can be seen that capacitor voltage ( $V_c$ ) is -10.5V, the DC-link voltage ( $U_o$ ) is 57V and inverter output phase voltage ( $V_g$ ) is 32.7V, respectively, which coincide well with the theoretical value. The negative voltage of capacitor represents that Z-source capacitor voltage is negative in upper and positive in lower, as shown in Fig. 3. Comparing Fig. 8(a) with Fig. 8(b), the DC-link voltage of traditional Z-source inverter is 66.5V. According to  $U_o = V_{dc}/(1-2D)$ , we can get  $D=24\%$ , i.e. the needed shoot-through duty ratio of IST-ZSI is smaller than the traditional one in the same inverter output. The capacitor voltage of traditional Z-source network is 50V and the maximum fluctuation at start can achieve 65V, which is much higher than IST-ZSI's.

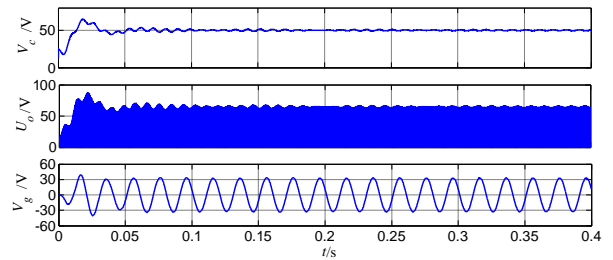


Fig.8. Comparison of waveforms between two topologies with the same output voltage. (a) IST-ZSI; (b) Traditional Z-source inverter.

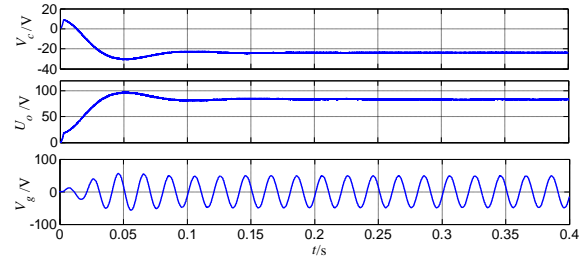


Fig.9. Simulation waveforms when  $D=30\%$ .

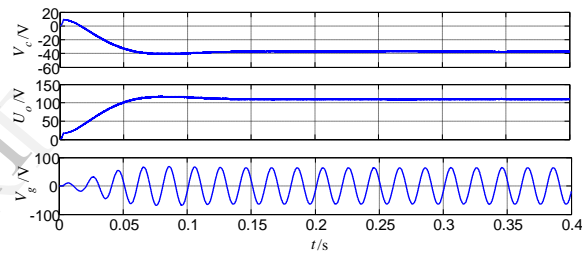


Fig.10. Simulation waveforms when  $D=35\%$ .

If continue increasing the shoot-through duty ratio of IST-ZSI, it is easy to get Fig. 9 and Fig. 10 which show the simulation waveforms of the capacitor voltage of Z-source network ( $V_c$ ), the DC-link voltage ( $U_o$ ) and three-phase voltage of inverter output ( $V_g$ ) when  $D=30\%$  and  $D=35\%$ , respectively.

The comparison between simulation results and theoretical values of  $V_c$ ,  $U_o$  and  $V_g$  in different shoot-through duty ratio can be seen in Tab. 2.

Tab.2. Comparison between simulation results and theoretical values in different shoot-through duty ratio

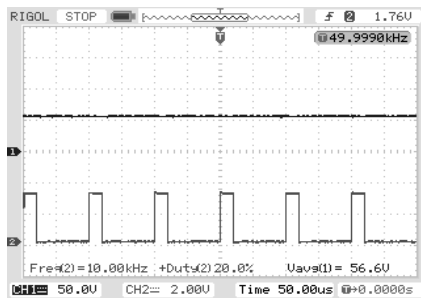
$D$		$V_c/V$	$U_o/V$	$V_g/V$
20%	Theoretical value	11.67	58.33	33.68
	Simulation value	10.5	57	32.7
30%	Theoretical value	26.25	87.5	50.52
	Simulation value	24	84.5	48.5
35%	Theoretical value	40.83	116.67	67.36
	Simulation value	38	112	64

It concludes, from Tab.2 and Fig. 8 to Fig. 10, the increasing shoot-through duty ratio results in the ascending of Z-source capacitor voltage, yet it is much lower than the capacitor voltage of traditional Z-source inverter. The DC-link voltage slowly increases, which becomes steady state in final. As boost factor and modulation index has realized decoupling control, the phase voltage of invert output is  $\sqrt{3}/3$  times of DC-link voltage, which is consistent with the actual

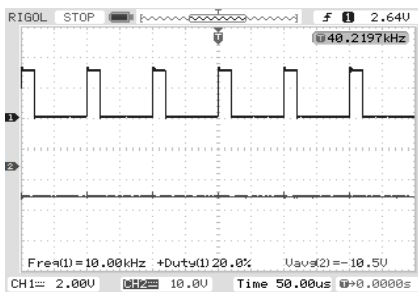
simulation results. Due to the impact of switching loss and the parasitic parameters, simulation value is lower than theoretical one after reaching steady state. However, compared with traditional Z-source inverter, the boost capability of IST-ZSI has improved a lot.

### V. EXPERIMENTAL VERIFICATION

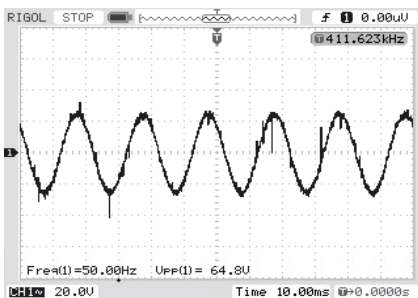
To further verify the correctness of isolated shoot-through Z-source inverter, a testing hardware circuit has been constructed. The same parameters as simulation are chosen to test the steady output waveforms of the DC-link voltage ( $V_o$ ), the capacitor voltage of Z-source network ( $V_c$ ) and the phase voltage of inverter output ( $V_g$ ) when  $D=20\%$ ,  $D=30\%$  and  $D=35\%$ . Figs. 11, 12 and 13 correspond to experimental results, respectively.



(a)

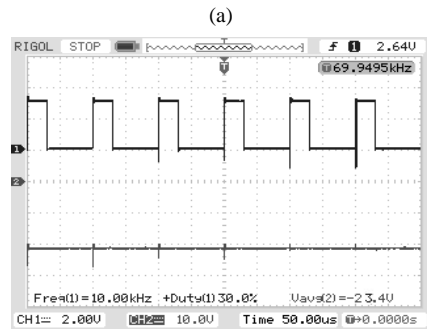
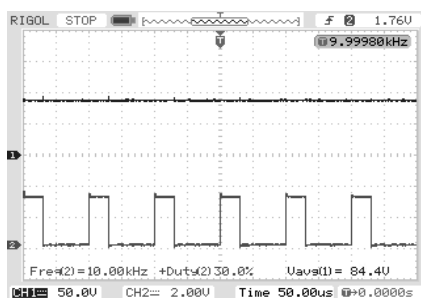


(b)

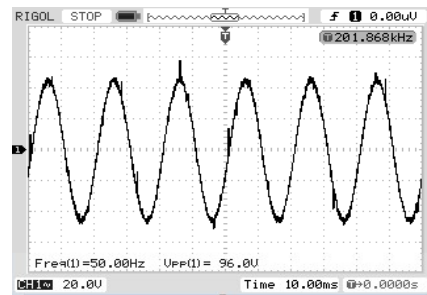


(c)

Fig.11 Experimental results when  $D=20\%$ . (a) DC-link voltage; (b) Capacitor voltage stress; (c) Phase voltage of inverter output.

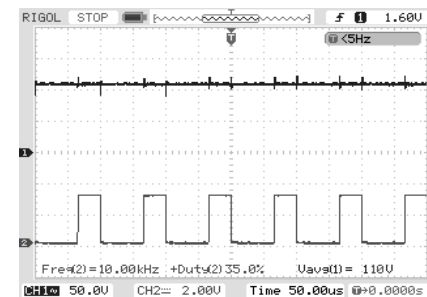


(b)

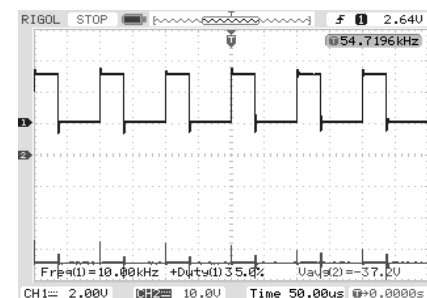


(c)

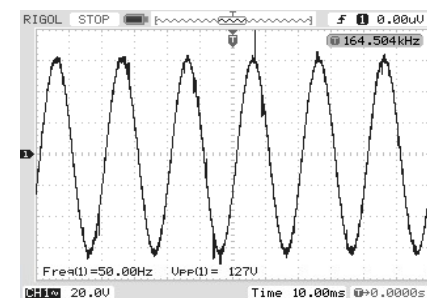
Fig.12. Experimental results when  $D=30\%$ . (a) DC-link voltage; (b) Capacitor voltage stress; (c) Phase voltage of inverter output



(a)



(b)



(c)

Fig.13. Experimental results when  $D=35\%$ . (a) DC-link voltage; (b) Capacitor voltage stress; (c) Phase voltage of inverter output

It can be seen from Fig. 11 to Fig. 13, when  $D=20\%$ ,  $D=30\%$  and  $D=35\%$ , the DC-link voltage ( $U_o$ ) is 56.6V, 84.4V and 110V, and capacitor voltage of impedance network ( $V_c$ ) is -10.5V, -23.4V and -37.2V, and the peak value of inverter output phase voltage is 64.8V, 96.0V and 127V, respectively. All experimental curves have a good agreement with the previous simulation and theoretical analysis results.

## VI. CONCLUSIONS

This paper has presented a novel Z-source inverter topology: isolated shoot-through Z-source inverter. The proposed inverter avoids the problem of serious starting-up inrush current and high capacitor voltage stress in traditional Z-source inverter. To overcome the mutual restriction of boost factor and modulation index, the control of shoot-through duty ratio is separated from the topology, which makes shoot-through duty ratio achieve flexibility control from 0 to 50% without the limitation of zero vectors in SPWM or SVPWM algorithm and improves the boost capability greatly. Therefore, the proposed inverter could be widely used in low input occasion. Both the simulation and experimental results demonstrate its feasibility and effectiveness.

## REFERENCES

- [1] Yang Shuitao, Ding Xinping, Zhang Fan, Qian Zhaoming. Study on Z-source Inverter for Photovoltaic Generation System[J]. Proceedings of the CSEE, 2008, 28(17): 112-118.
- [2] Wang Jidong, Zhu Xueling, Su Haibin, Wang Linghua. Proportional-resonant control for Z-source inverter in three-phase PV grid-connected system[J]. Electric Machines and Control, 2010, 14(4): 86-91.
- [3] Zheng Jianyong, Huang Jinjun, You Jun, Zhang Xianfei, Zhang Xiaowen. Research on Z source based current hysteresis control used in photovoltaic grid-connected system[J]. Electric Machines and Control, 2010, 14(5): 61-67.
- [4] Liu Heping, Lin Ping, Hu Yinquan, Fu Qiang. Control Scheme of Bi-Directional Z-Source Inverter in Improving the Dynamic Performance of Electrical Vehicles[J]. Transactions of China Electrotechnical Society. 2012, 27(2): 139-145.
- [5] Peng Fangzheng, Shen Miaosen, Holland Kent. Application of Z-Source Inverter for Traction Drive of Fuel Cell-Battery Hybrid Electric Vehicles[J]. IEEE Transactions on Power Electronics, 2007, 22(3): 1054-1061.
- [6] Peng Fangzheng, Joseph Alan, Wang Jin, Shen Miaosen, et al.. Z-Source Inverter for motor Drives[J]. IEEE Transactions on Power Electronics, 2005, 20(4): 857-863.
- [7] Fang Xupeng. Three-Phase Current-Fed-Z-Source AC/AC Converter for Motor Drives[J]. Transaction of China Electrotechnical Society, 2007, 22(7): 165-168.
- [8] Loh Poh Chiang, Lim Sok Wei, Gao Feng, Blaabjerg Frede. Three-Level Z-Source Inverters Using a Single LC Impedance Network[J]. IEEE Transactions on Power Electronics, 2007, 22(2): 706-711.
- [9] Zhang Lunjian, Tan Guojun, Chen Liping. Neutral-point potential balance control for three-level Z-source inverters based on double modulation wave technique[J]. Power System Protection and Control, 2013, 41(7): 91-96.
- [10] Kominami Tsutomu, Fujimoto Yasutaka. A Novel Nine-Switch Inverter for Independent Control of Two Three-phase Loads[C]. Industry Applications Conference, September 23-27, 2007. New Orleans, LA, 2007: 2346-2350.
- [11] Anderson Joel, Peng F. Z.. Four Quasi-Z-Source Inverters[C]. IEEE Power Electronics Specialists Conference: PESC, June 15-19, 2008: 2743-2749.
- [12] Strzelecki Ryszard, Adamowics Marek, Strzelecka Natalia, Bury Wieslaw. New Type T-Source Inverter[C]. Compatibility and Power Electronics: CPE, May 20-22, 2009. Badajoz, 2009: 191-195.
- [13] Zhou Yufei, Huang Wenxin, Zhao Jianwu, Zhao Ping. Tapped Inductor Quasi-Z-source Inverters[J]. Proceedings of the CSEE, 2012, 32(27): 126-134.
- [14] Nguyen Minh-Khai, Lim Young-Cheol, Cho Geum-Bae. Switched-Inductor Quasi-Z-Source Inverter[J]. IEEE Transactions on Power Electronics, 2011, 26(11): 3183-3191.
- [15] Peng Fangzheng. Z-source inverter[J]. IEEE Transactions on Industry Applications, 2003, 39(2): 504-510.
- [16] Zhu Miao, Yu Kun, Luo Fang Lin. Switched Inductor Z-Source Inverter[J]. IEEE Transactions on Power Electronics, 2010, 25(8): 2150-2158.
- [17] Tang Yu, Xie Shaojun, Zhang Chaohua. Improved Z-source Inverter[J]. Proceedings of the CSEE, 2009, 29(30): 28-34.
- [18] Tang Yu, Xie Shaojun, Zhang Chaohua, Xu Zegang. Improved Z-source inverter with reduced Z-source capacitor voltage stress and soft-start capability[J]. IEEE Transactions on Power Electronics, 2009, 24(2):409-415.
- [19] Zhang Chaohua, Tang Yu, Xie Shaojun. Third Harmonic Injection Control Strategy of Improved Z-Source Inverter[J]. Transaction of China Electrotechnical Society, 2009, 24(11): 114-127.
- [20] Gajanayake Chandana Jayampathi, Luo Fang Lin, Gooi Hoay Beng, So Ping Lam, Siow Lip Kian. Extended-Boost Z-Source Inverters[J]. IEEE Transactions on Power Electronics, 2010, 25(10):2642-2652.
- [21] Li Ding, Loh Poh Chiang, Zhu Miao, Blaabjerg Frede. Hybrid-Source Impedance Networks: Layouts and Generalized Cascading Concepts[J]. IEEE Transactions on Power Electronics, 2011, 26(7): 2028-2040.
- [22] Miao Zhu, Kun Yu, Fang Lin Luo. Switched Inductor Z-Source Inverter[J]. IEEE Transactions on Power Electronics, 2010, 25(8): 2150-2158.